



Composition Investigations of Nearly Lattice-Matched InGaPN Films on GaAs (001) Substrates Grown by MOVPE

Phongbandhu Sritonwong [a], Sakuntam Sanorpim* [a,b], Kentaro Onabe [c]

[a] Nanoscience and technology, Graduate School, Chulalongkorn University, Phatumwan, Bangkok 10330, Thailand.

[b] Department of Physics, Faculty of Science, Chulalongkorn University, Phatumwan, Bangkok 10330, Thailand.

[c] Department of Advanced Materials Science, The University of Tokyo, Kashiwanoha, Kashiwa, Chiba 277-8561, Japan.

*Author for correspondence; e-mail: Sakuntam.s@chula.ac.th

Received: 15 September 2015

Accepted: 6 November 2015

ABSTRACT

We have reported on an alternative way, which is a combination of micro-Raman spectroscopy and high resolution X-ray diffraction (HRXRD) measurements, to evaluate the In and N contents and a corresponding misfit strain in the InGaPN films grown on GaAs (001) substrates by metal organic vapor phase epitaxy (MOVPE). Firstly, the In content was evaluated by means of micro-Raman scattering to be 56.4 ± 0.8 at%, 55.8 ± 0.8 at%, 55.9 ± 0.9 at% and 55.7 ± 1.1 at%, which were confirmed by HRXRD, for the DMHy flow rates of 0, 300, 700 and 1,100 $\mu\text{mol}/\text{min}$, respectively. Based on HRXRD results, next, the N content was estimated to be 0.9 ± 0.4 at%, 1.4 ± 0.4 at% and 2.1 ± 0.5 at% for the DMHy flow rates of 300, 700 and 1,100 $\mu\text{mol}/\text{min}$, respectively. With increasing N content, misfit strain is also reduced from 0.65% to 0.12%. This suggests that a nearly lattice-matched film, which has the highest N content of 2.1 ± 0.5 at%, exhibits the lowest misfit strain of 0.12%. Our results showed an achievement in a use of micro-Raman spectroscopy as a tool to evaluate the In content, which is a primary parameter using to calculate the N content in the InGaPN film.

Keywords: MOVPE, HRXRD, Raman scattering, InGaPN, III-V Nitrides, misfit strain, lattice mismatch

1. INTRODUCTION

InGaPN is an interesting dilute nitride due to the tunable structural and optical properties. Its lattice constant can be lattice-matched to various substrates, such as GaAs [1, 2] and GaP [3, 4] by adjusting the indium

(In) and nitrogen (N) contents. A huge bowing parameter, which is a characteristic of the dilute III-V-Nitrides, can cause a large reduction of bandgap with a small amount of the N incorporation [4, 5]. On the other

hand, These tunable properties, both lattice constant and bandgap, are made InGaPN to suitable in many applications, such as a multi-junction solar cells [1, 2], light emitting diodes (LEDs) [1, 6, 7], lasers and heterojunction bipolar transistors [1, 2].

One of the challenges of InGaPN compared to the N-free InGaP is the method to examine the In content. It is due to a change of In incorporation, inducing by a present of N-precursor during the MOVPE growth [8]. For InGaP, high resolution X-ray diffraction (HRXRD) is commonly used to verify the In content associated by the interpolation owing to Vegard's law [8, 9, 10]. On the other hand, for InGaPN, HRXRD cannot directly apply to evaluate both the In and N contents in the same time. Since, due to the variation of four elements in InGaPN, the In content is required as a key parameter for calculation of N content. However, the In content is an unknown parameter, which is possibly effected by an introduction of N [8]. Thus, to determine the N content, the In content is need to be firstly confirmed by other methods, such as secondary ion mass spectrometry (SIMS) [8, 11].

Recently, micro-Raman spectroscopy was used as a tool to evaluate the In content in InGaP, which is attributed to a shift of GaP-like LO phonon [12]. In this work, due to a small amount of N incorporation, Raman scattering technique associated with HRXRD has been applied to evaluate the In content in InGaPN, which is a primary parameter to examine the N content. Besides, the misfit strain dependent on the N incorporation also have been investigated.

2. EXPERIMENTAL DETAILS

$\text{In}_x\text{Ga}_{1-x}\text{P}_{1-y}\text{N}_y$ films were grown on GaAs (001) substrates by metalorganic vapor phase epitaxy (MOVPE) with trimethylgallium (TMGa), trimethylindium

(TMIn), tertiarybutylphosphine (TBP), tertiarybutylarsine (TBAs) and dimethylhydrazine (DMHy) as a precursors of Ga, In, P As and N, respectively. Pressure and total flow rate were kept at 60 Torr and 2000 sccm, respectively. Before the InGaPN growth, the GaAs substrate was thermally cleaned at 650°C in TBAs atmosphere for 15 min. A 100-nm-thick GaAs layer grown at 650°C is used as a buffer. Growth temperature and growth time of InGaPN were 520°C and 10 min, respectively. To obtain the $[\text{TMIn}]/([\text{TMIn}]+[\text{TMGa}])$ mole fraction of 0.63, flow rates of TMIn and TMGa were respectively kept at 14.7 and 8.6 $\mu\text{mol}/\text{min}$ for all the samples. Since, the $[\text{TMIn}]/([\text{TMIn}]+[\text{TMGa}])$ mole fraction of 0.63 is expected to make the compressive strain in the grown layer. To compensate the compressive strain, the N content was increased by varying DMHy flow rates in the range of 0-1,100 $\mu\text{mol}/\text{min}$.

All the grown films were morphologically characterized by atomic force microscopy (AFM) and scanning electron microscopy (SEM). Based on HRXRD measurements, both a symmetric (004) $2\theta/\omega$ -scan and an asymmetric (115) reciprocal space map (RSM) were carried out to investigate lattice parameters, normal (a_{\perp}) and in-plane (a_{\parallel}) lattice parameters, and a misfit strain for the InGaPN films as dependent on DMHy flow rate. Micro-Raman technique was employed to analyze the In incorporation in InGaPN as well as in the N-free InGaP. The 514.5 nm line of an Ar⁺ laser with excitation spot of about 2 μm was used as a source of Raman excitation. The peak shift is quite uniform when measurements were taken at several locations of the InGaPN film. With a combination of HRXRD and Micro-Raman spectroscopy measurements, the N content in all the InGaPN films was

quantitatively analyzed.

3. RESULTS AND DISCUSSION

The growth of InGaPN films on GaAs (001) substrates were established by HRXRD analysis using a symmetrical (004) $2\theta/\omega$ scan and an asymmetrical (115) reciprocal lattice mapping (RSM). Figure 1 shows HRXRD (004) $2\theta/\omega$ profiles of InGaPN films with different DMHy flow rates of (a) 0, (b) 300, (c) 700 and (d) 1,100 $\mu\text{mol}/\text{min}$. All the diffraction pattern consists of a well-defined diffraction peak located at 66.06° , which is referred to the GaAs (004) reflection and a broaden curve at lower diffraction angles, indicating the (In)GaPN (004) reflections. Compared to the N-free InGaP film, the InGaPN (004) reflection peak shifts from 65.45° to the higher angles with increasing DMHy flow rates. This shows a reduction of the normal lattice parameter (a_\perp) due to the N incorporation. Besides, an increase of full width at half maximum (FWHM) with increasing DMHy flow rate is also clearly seen, demonstrating a less coherency of lattice spacing due to a large distribution of both the In and N contents in the InGaPN layers.

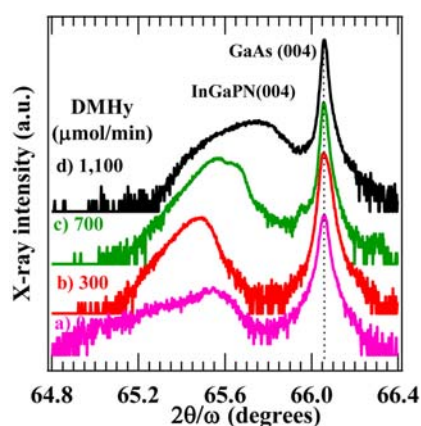


Figure 1. HRXRD $2\theta/\omega$ profiles of (a) InGaP film and (b) - (d) InGaPN films grown on GaAs (001) substrates with a constant $[\text{TMIn}]/([\text{TMIn}]+[\text{TMGa}])$ ratio of 0.63 as dependent on DMHy flow rates.

Figure 2 shows HRXRD reciprocal space maps taken around an asymmetric (115) reflection of (a) the N-free InGaP film and (b) - (c) the InGaPN films as dependent on the DMHy flow rate. It is seen that diffraction from both GaAs (115) and InGaPN (115) planes are clearly observed. The separation between the GaAs and InGaPN diffraction contours in ω -axis, " $\Delta\omega$ ", is corresponded to a tilt angle between the GaAs (115) and InGaPN (115) planes. It is noted that $\Delta\omega$ will be become zero for a fully relaxed film, which results in parallel GaAs (115)//InGaPN (115) planes. Then again, the diffraction contours of GaAs (115) and InGaPN (115) planes are aligned along the fully strained line (dashed line), when the film exhibits as a coherently grown film, resulting in lattice-matching between lattice constant of GaAs and in-plane lattice parameter (a_\parallel). Thus, the grown film is under a fully strain condition. On the other hand, the separation in $2\theta/\omega$ -axis is resulted from the difference in lattice spacing, which is reduced with increasing DMHy flow rate. Furthermore, a rotation of the elliptic contour of the InGaPN (115) indicates an existence of a residual strain in the film. It is evidenced that, for the highest DMHy flow rate of 1,100 $\mu\text{mol}/\text{min}$, the InGaPN film is still under a compressive strain condition.

Figure 3 (a) shows a typical surface morphology of the InGaPN film grown on GaAs (001) substrate with the highest DMHy flow rate of 1,100 $\mu\text{mol}/\text{min}$ observed by AFM with a scanning area of $10 \times 10 \mu\text{m}^2$. It is clear that the surface of all the InGaPN films shows the island-like features with an elliptic shape, which is aligned in an elongate the [110] direction. For the highest DMHy flow rate, root means square (RMS) roughness was observed to 25.2 nm. A formation of the elliptic shaped structure may be resulting from decreasing of

a migration length due a large value of $[TMIn]/([TMIn]+[TMGa])$ as well as a presence of DMHy during the growth. Figures 1 (b) and 1(c) show cross-sectional SEM images of the corresponding InGaPN film with thickness of about $0.7 \mu\text{m}$ taken with secondary electron imaging (SEI) and back-scattering imaging modes,

respectively. Abrupt interface between InGaPN film and GaAs substrate are clearly observed even though the DMHy flow rate as high as $1,100 \mu\text{mol}/\text{min}$. This indicates a high quality interface, which is avoided from a strain relaxation at the interface, due to a small amount of misfit strain.

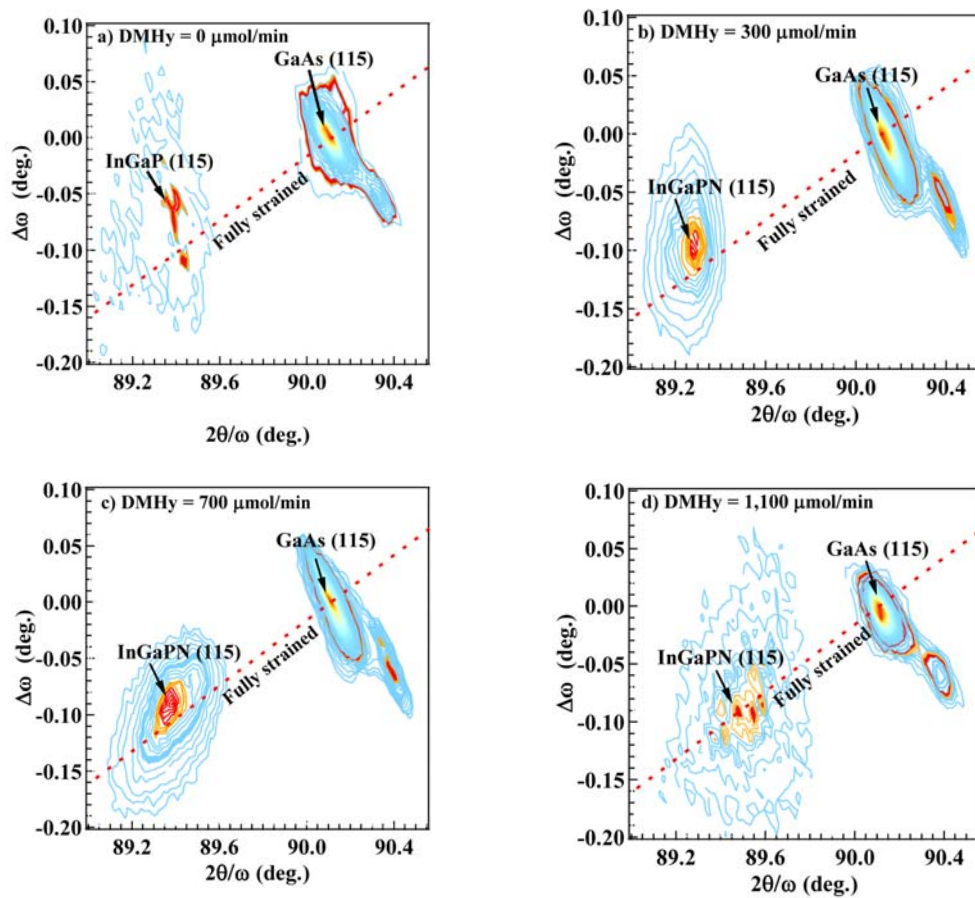


Figure 2. HRXRD $2\theta/\omega$ and $\Delta\omega$ reciprocal space maps around an asymmetrical (115) reflection for the InGaPN films on GaAs(001) substrates as dependent on the DMHy flow rates, (a) 0, (b) 300, (c) 700 and (d) $1,100 \mu\text{mol}/\text{min}$.

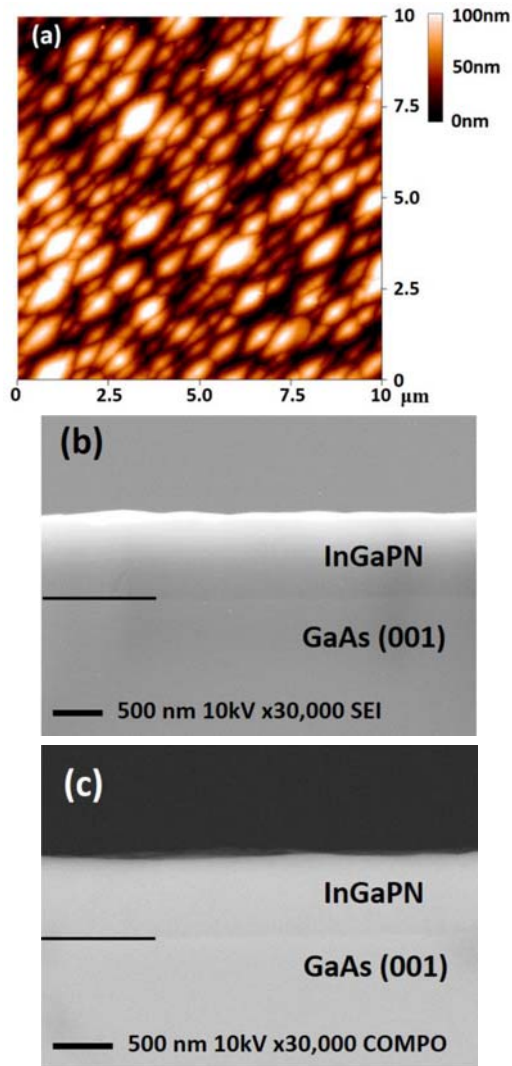


Figure 3. (a) AFM image (10 μm scale) of surface of InGaPN film on GaAs (001) substrate with the highest DMHy flow rate of 1,100 $\mu\text{mol}/\text{min}$. Cross-sectional SEM images taken with (b) a secondary electron imaging (SEI) and (c) a back-scattering imaging modes of the corresponding InGaPN film.

To analyze the In content, relaxed lattice constant (a), lattice mismatch and misfit strain in the N-free InGaP film, values of a and ϵ were firstly determined by a symmetric (004) $2\theta/\omega$ -scan and an asymmetric (115) RSM. According to Vegrad's law [8, 9 10], the

In content and ϵ were determined using the initial input parameters listed in Table 1. The values of a and ϵ of the N-free InGaP film are listed in Table 2. Thus, the In content and value of ϵ were calculated to $56.6 \pm 1.7 \text{ at}\%$ and $5.65 \pm 0.01 \text{ \AA}$, respectively. A large variation of In content ($\pm 1.7 \text{ at}\%$) is due to a distribution of In concentration, which is larger than an instrumental error. The misfit strain in InGaP layer was evaluated to be 0.65%. Unfortunately, for the N-contained InGaPN films, the N content cannot be evaluated with using only the results obtained from HRXRD. It is due to a combination of four elements in such quaternary InGaPN alloy. Therefore, to calculate the N content, the In content is needed to be initially confirmed by another method that we selected micro-Raman scattering technique.

Figure 4(a) shows Raman spectrum of the N-free InGaP film on GaAs (001) substrate. The spectrum consists of three features located at the wave number of about 380, 360 and 330 cm^{-1} , which are attributed to GaP-like LO, InP-like LO and InP-like TO phonons, respectively. It is well known that the In content in InGaP is significantly related to the optical phonon frequencies, especially GaP-like LO phonon reported by Bedel et al.[13]. A shift of GaP-like LO phonon frequency ($\Delta\omega_{\text{GaP-like LO}}$) as a function of the In content (x) is expressed as

$$\Delta\omega_{\text{GaP-like LO}} = -18.18x^2 - 38.97x. \quad (1-1)$$

Here $Dw_{\text{GaP-like LO}}$ is a different between the frequencies of GaP-like LO phonon taken from InGaP compared to that of GaP-LO phonon taken from GaP (404.99 cm^{-1}). Therefore, we used the value of $w_{\text{GaP-like LO}}$ taken from the N-free InGaP film, as shown in Figure 4(a) to calculate the In content to be $56.4 \pm 0.8 \text{ at}\%$. This result agrees well with that of HRXRD. Unlike the

variation of In content (± 1.7 at%) obtained from HRXRD, the value of ± 0.8 at% obtained from micro-Raman scattering

represents an error, which is introduced by a step size in wave-number axis.

Table 1. Relaxed lattice constant (a) and elastic constants (C_{11} and C_{12}) of GaP, cubic-GaN, InP and cubic-InN. C_{11} and C_{12} are in unit of 10^{11} dyn/cm².

Parameters	GaP	Cubic-GaN	InP	Cubic-InN
a_0 (Å)	5.450 ^[14]	4.503 ^[15]	5.868 ^[16]	4.98 ^[15]
C_{11}	14.12 ^[17]	26.4 ^[15]	10.22 ^[18]	17.2 ^[19]
C_{12}	6.253 ^[17]	15.3 ^[15]	5.76 ^[18]	11.9 ^[19]

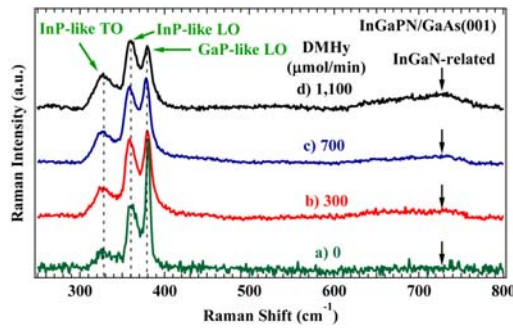


Figure 4. Raman spectra of InGaPN films grown on GaAs (001) substrates with various DMHy flow rates rates of (a) 0, (b) 300, (c) 700 and (d) 1,100 $\mu\text{mol}/\text{min}$.

Figures 4(b)-4(d) illustrate Raman spectra of InGaPN films grown on GaAs (001) substrates with various DMHy flow rates of (b) 300, (c) 700 and (d) 1,100 $\mu\text{mol}/\text{min}$. The GaP-like LO, InP-like LO and InP-like TO phonons are also observed for all the InGaPN films. In addition, another broad feature related to N incorporation was observed at wave number around 730 cm^{-1} . With increasing DMHy flow rate, its intensity is significantly increased, indicating a higher amount of N incorporation into the InGaPN film. This feature is known as the InGaN-related local vibrational mode [9]. According to GaP-like LO phonon frequencies, the In content in the InGaPN films was determined to 55.8 ± 0.8 at%,

55.9 ± 0.9 at% and 55.7 ± 1.1 at% for the DMHy flow rates of 300, 700 and 1,100 $\mu\text{mol}/\text{min}$, respectively. It is seen that the In content in InGaPN is slightly lower than that in the N-free InGaP. This difference is due to a modification of a misfit strain in the N-contained InGaPN films [6]. With a use of the In content calculated using the shift of GaP-like LO phonon and the normal (a_{\perp}) and in-plane (a_{\parallel}) lattice parameters obtained from HRXRD measurements, the N content in the InGaPN films can be acquired by the modified Vegard's law [8, 9, 10],

$$a_{\text{InGaPN}} = \frac{2 \cdot C_{12} \cdot a_{\parallel} + C_{12} \cdot a_{\perp}}{2 \cdot C_{12} + C_{11}} \quad (1-2)$$

$$a_{\text{InGaPN}} = (1-x)[(1-y)a_{\text{GaP}} + ya_{\text{GaN}}] + x[(1-y)a_{\text{InP}} + ya_{\text{InN}}] \quad (1-3)$$

$$C_{11} = \frac{(1-x)[(1-y)a_{\text{GaP}}C_{11}^{\text{GaP}} + ya_{\text{GaN}}C_{11}^{\text{GaN}} + x[(1-y)a_{\text{InP}}C_{11}^{\text{InP}} + ya_{\text{InN}}C_{11}^{\text{InN}}]}{a_{\text{InGaPN}}} \quad (1-4)$$

$$C_{12} = \frac{(1-x)[(1-y)a_{\text{GaP}}C_{12}^{\text{GaP}} + ya_{\text{GaN}}C_{12}^{\text{GaN}} + x[(1-y)a_{\text{InP}}C_{12}^{\text{InP}} + ya_{\text{InN}}C_{12}^{\text{InN}}]}{a_{\text{InGaPN}}} \quad (1-5)$$

where C_{11} and C_{12} are the elastic constants $\text{In}_x\text{Ga}_{1-x}\text{P}_{1-y}\text{N}_y$ and a_{GaP} , a_{GaN} , a_{InP} and a_{InN} are

the relaxed lattice constants of cubic GaN, GaP, InP and cubic InN, respectively (see Table 1). Since the elastic constants of $\text{In}_x\text{Ga}_{1-x}\text{P}_{1-y}\text{N}_y$ are not available, they can, thus, be derived from the elastic constants of the four binary compounds by using the interpolation scheme. The N content and the misfit strain of InGaPN films were evacuated, as show in Figure 5 and Table 2. Figure 5 shows a plots of the N and In contents as dependent on DMHy flow rate. With increasing DMHy flow rate from 0 to 1,100 $\mu\text{mol}/\text{min}$, the N content is increased from 0 to 2.1 ± 0.5 at%.

It is observed that, as the highest N content of 2.1 ± 0.5 at%, the InGaPN grown layer is became a nearly lattice-matched film with the lowest misfit strain of 0.12%, which is about five times smaller than that of the N-free InGaP film. It is known that the lattice-matching condition between film and substrate prevents the epitaxial layer from a

misfit dislocation, which degrade the quality of the grown layer. A nearly lattice-matched InGaPN on GaAs with a good quality were coherently grown by MOVPE with the In and N contents of 55.7 ± 1.1 at% and 2.1 ± 0.5 at%, respectively.

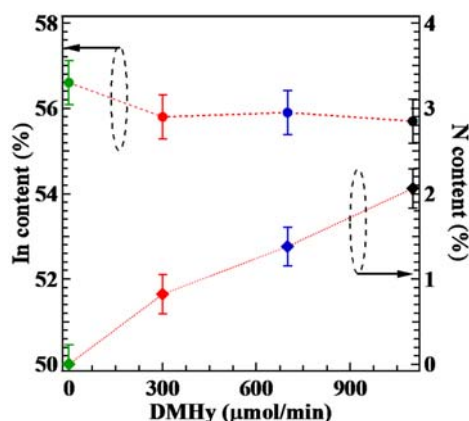


Figure 5. The In and N content of the InGaPN films as dependent DMHy flow rates grown with $[\text{TMIIn}]/([\text{TMIIn}]+[\text{TMGa}])$ ratio of 0.63.

Table 2. Relaxed lattice constant (a), misfit strain (ϵ_{\parallel}) and In content determined by micro-Raman spectroscopy) and calculated N content. Noted that the In content determined by HRXRD is 56.6 ± 1.7 at%.

[DMHy] ($\mu\text{mol}/\text{min}$)	GaP-LO (cm^{-1})	a_{\perp} (\AA)	a_{\parallel} (\AA)	a_{\circ} (%)	Misfit strain (%)	In (at%)	N (at %)
0	378.2 ± 0.5	5.71	5.67	5.69	0.65	56.4 ± 0.8	-
300	378.7 ± 0.5	5.70	5.66	5.68	0.47	55.8 ± 0.8	0.9 ± 0.4
700	378.6 ± 0.6	5.69	5.65	5.67	0.30	55.9 ± 0.9	1.4 ± 0.4
1,100	378.7 ± 0.6	5.67	5.65	5.66	0.12	55.7 ± 1.1	2.1 ± 0.5

4. CONCLUSIONS

A combination of HRXRD and Raman spectroscopy measurements has been proposed to evaluate the In and N contents in the nearly lattice-matched InGaPN films grown on GaAs (001) substrates. According to Raman scattering results, the In content was calculated to be 56.4 ± 0.8 at%, 55.8 ± 0.8 at%, 55.9 ± 0.9 at% and 55.7 ± 1.1 at% for InGaPN films with DHMy flow rates of

0, 300, 700 and 1,100 $\mu\text{mol}/\text{min}$, respectively. Then, the N contents, which was successfully calculated using an interpolation method via Vergrad' law, are 0.9 ± 0.4 at%, 1.4 ± 0.4 at% and 2.1 ± 0.5 at% for the InGaPN films with DMHy flow rates of 300, 700 and 1,100 $\mu\text{mol}/\text{min}$, respectively. An incorporation of N significantly influenced on a misfit strain in the InGaPN films, which is significantly reduced with increasing N

content. We achieved a nearly lattice-matched InGaPN film to GaAs with the lowest magnitude of misfit strain of 0.12%.

ACKNOWLEDGMENTS

This research has been supported by the Ratchadaphiseksomphot Endowment Fund of Chulalongkorn University (RES560530229-EN) and the 90th Anniversary of Chulalongkorn University Fund (the Ratchadaphiseksomphot Endowment Fund).

REFERENCES

- [1] Kaewket D., Sanorpim S., Tungasmita S., Katayama R. and Onabe K., *Phys. Status Solidi C*, 2010; **7**: 2079-2081.
- [2] Hong Y.G., André R. and Tu C.W., *J. Vac. Sci. Technol.*, 2001; **B 19**, 1413.
- [3] Onabe K., Kimura T., Nakadan C., Wu J., Ito Y., Yoshida S., Kikawa J. and Shiraki Y., presented in ICCG-13/ICVGE-11, Kyoto (2001).
- [4] Kaewket D., Tungasmita S., Sanorpim S., Katayama R. and Onabe K., *Adv. Mater. Res.*, 2008; **55-57**: 821-824.
- [5] Tu C.W., Chen W.M., Buyanova I.A. and Hwang J.S., *J. Cryst. Growth*, 2006; **288**: 7-11.
- [6] Xin H.P., Weltry R.J., Hong Y.G. and Tu C.W., *J. Cryst. Growth*, 2001; **227-228**: 558-561.
- [7] Odnoblyudov V.A. and Tu C.W., *Appl. Phys. Lett.*, 2006; **89**: 191107.
- [8] Sanorpim S., Nakajima F., Nakandan N., Kimura T., Katayama R., Onabe K., *J. Cryst. Growth*, 2005; **275**: e1017-e1021.
- [9] Lin K.I., Lee J.Y., Wang T.S., Hsu S.H., Hwang J.S., Hong Y.G. and Tu C.W., *Appl. Phys Lett*, 2005; **86**: 211914.
- [10] Wang T.S., Lin K.I. and Hwang J.S., *J. Appl. Phys*, 2006; **100**: 093709.
- [11] Kaewket D., Sanorpim S., Tungasmita S., Katayama R. and Onabe K., *Physica E*, 2010; **42**: 1176-1179.
- [12] Lee H., Biswas D., Klein M.V., Morkoc H., Aspnes D.E., *J. Appl. Phys*, 1994; **75**: 5040.
- [13] Bedel E., Carles R., Landa G. and Renucci J.B., *Rev. Phys. Appl*, 1984; **B30**: 5923.
- [14] Sanorpim S., Structural and Optical properties of III-III-V-N Type A;oy Films and Their Quantum Wells., PhD Thesis, The University of Tokyo, Japan, 2003.
- [14] Besslov N.V., Dedegkrev T.T., Efimov A.N., Kartenko N.F. and Yakovlev YuP., *Sov. Phys. Solid State (English Transl.)*, 1980; **22**: 1652.
- [15] Sell D.D., Casey H.C., Wecht K.W., *J. Appl. Phys*, 1974; **45**: 2650.
- [16] Giesecke G., Pfister H., *Acta Crystallogr*, 1958; **11**: 369.
- [17] Bugajski M., Lewandowski W.J., *J. Appl. Phys*, 1985; **57**: 521.
- [18] Hickernell F.S. and Gayton W.R., *J. Appl. Phys*, 1966, **37**: 462.
- [19] Sherwin M.E. and Drummond T.J., *J. Appl. Phys*, 1991; **69**: 8423.
- [20] Jahne E., Pilz Giehler W. and Hildish L., *Phys. Status Solidi*, 1979; **B 91**: 155-165.
- [21] Kim K.M., Nonoguchi S., Krishnamurthy D., Emura S., Hasegawa S. and Asahi H., *J. appl. physics*, 2012; **112**: 063507.
- [22] Yoon S.F., Mah K.W., Zheng HQ., Gay B.P. and Zhang P.H., *Microelectronics Journal*, 2000; **31**: 15-21.